

# Spin transfer switching in the nanosecond regime for CoFeB/MgO/CoFeB ferromagnetic tunnel junctions

著者	安藤 康夫
journal or publication title	Journal of Applied Physics
volume	103
number	10
page range	103911-1-103911-4
year	2008
URL	<a href="http://hdl.handle.net/10097/46556">http://hdl.handle.net/10097/46556</a>

doi: 10.1063/1.2930873

# Spin transfer switching in the nanosecond regime for CoFeB/MgO/CoFeB ferromagnetic tunnel junctions

Tatsuya Aoki,<sup>1,a)</sup> Yasuo Ando,<sup>1</sup> Daisuke Watanabe,<sup>1</sup> Mikihiro Oogane,<sup>1</sup> and Terunobu Miyazaki<sup>2</sup>

<sup>1</sup>Graduate School of Engineering, Tohoku University, Aoba-yama 6-6-05, Sendai 980-8579, Japan

<sup>2</sup>WPI Advanced Institute for Materials Research, Tohoku University, Aoba-yama 6-6-04, Sendai 980-8579, Japan

(Received 6 February 2008; accepted 28 March 2008; published online 28 May 2008)

Detailed spin transfer switching properties in the nanosecond region for CoFeB/MgO(001)/CoFeB magnetic tunnel junctions are reported. The switching current ( $I_C$ ) was greatly increased in the  $<10$  ns region. This characteristic resembles that of current-perpendicular-to-plane giant magnetoresistance (CPP-GMR), although both the junction geometry and resistance differ from those of a CPP-GMR device. We discussed the switching properties considering the contribution of high frequency loss and the theoretical limitation of the analytical model. Furthermore, we observed real-time switching in the nanosecond region. Using these results, we discuss the spin transfer switching mechanism in the nanosecond region with both adiabatic and thermally activated models. © 2008 American Institute of Physics. [DOI: 10.1063/1.2930873]

## I. INTRODUCTION

Giant tunnel magnetoresistance (TMR) effect in magnetic tunnel junctions (MTJs) with a MgO(001) tunnel barrier,<sup>1,2</sup> especially that of a CoFeB/MgO/CoFeB system,<sup>3</sup> promises the advancement of industrial applications for magnetoresistive random access memory (MRAM) and magnetic sensors. When electric current passes through a nanoscale MTJ, the reference layer creates spin-polarized current, which can exert torque on free layer magnetization.<sup>4–6</sup> This torque can reverse the free layer magnetization if the amount of the spin current is sufficient, which is so-called spin transfer switching (STS). Actually, STS is expected to reduce the necessary writing current of a MRAM unit cell to a level that is lower than that necessary for inductive-field writing method, especially for cell widths of less than 100 nm. In CoFeB/MgO/CoFeB MTJs, STS has been observed by several groups.<sup>7–10</sup> The switching current density  $J_C$  of  $\sim 10^6$ – $10^7$  A/cm<sup>2</sup> and log-linear-like dependence on switching time  $\tau_p$  in the  $\tau_p > 10$  ns region are explained using a thermal activation model.<sup>11,12</sup> On the other hand, in the  $\tau_p < 10$  ns region,  $J_C$  increases drastically with decreased  $\tau_p$ .<sup>10,13</sup> That increasing characteristic was reported also for current-perpendicular-to-plane giant magnetoresistance (CPP-GMR) systems,<sup>11,14–17</sup> in which the drastic increase was explained by adiabatic precession amplification attributable to spin transfer torque.<sup>18</sup> However, that mechanism is not thoroughly understood. Additionally, differences must exist between the spin transfer mechanisms of CPP-GMR and MTJ. In a previous report of experiments,<sup>10</sup> the critical current  $I_C$  was 200–600  $\mu$ A, corresponding to the bias voltage of several hundred millivolts. In MTJ, it is theoretically predicted that the transport mechanism is complex and depends on the bias voltage.<sup>19,20</sup> From a different perspective,

the drastic increase in  $I_C$  with reduced  $\tau_p$  in the nanosecond region can also be explained by other effects such as high frequency loss and theoretical limitation.

This paper presents descriptions of both conventional static pulsed current versus resistance ( $I$ – $R$ ) measurement<sup>7,9,10,13</sup> and real-time observation of the switching process directly on the same MTJ. Using the static technique, we consider the influence of the additional effects on  $I_C$  under various switching times. For the dynamic one, similar experiments have already been reported.<sup>21–23</sup> Some of them examined the properties of CPP-GMR (Refs. 21 and 22) and described steady state precession<sup>22</sup> or random telegraph switching<sup>21,22</sup> in the region where the resistance was reversible for the current amplitude. Another experiment<sup>23</sup> used CoFeB/MgO/CoFeB MTJ and observed STS in the region where the resistance was irreversible for the current amplitude. However, the MR ratio of the MTJ was not so high even for CoFeB/MgO/CoFeB structure. In this paper, we present STS data for a P to AP switching event at room temperature for one CoFeB/MgO/CoFeB junction, which exhibits a 115% MR ratio, which ensures the reliability of the experiment.

## II. METHOD

The structure of MTJs used in this study is Ta/Py/IrMn/Co<sub>90</sub>Fe<sub>10</sub>/Ru/Co<sub>40</sub>Fe<sub>40</sub>B<sub>20</sub>/MgO/Co<sub>40</sub>Fe<sub>40</sub>B<sub>20</sub>/Ta/Ru on a 1  $\mu$ m thermally oxidized Si wafer using an UHV magnetron sputtering system. The Co<sub>40</sub>Fe<sub>40</sub>B<sub>20</sub> free layer thickness is 2 nm. The MTJ was patterned using electron-beam lithography and Ar ion milling into a 110  $\times$  330 nm<sup>2</sup> elliptical shape. The electrode was patterned into a coplanar waveguide with very low capacitance for ultrafast pulsed current transmittance.<sup>24</sup> The MTJ was annealed at 270 °C for 1 h in a 5 kOe magnetic field. A static pulsed current versus resistance measurement was performed using an ac two probe method. We prepared two different circuits depending on the

<sup>a)</sup>Electronic mail: aoki@mlab.apph.tohoku.ac.jp.

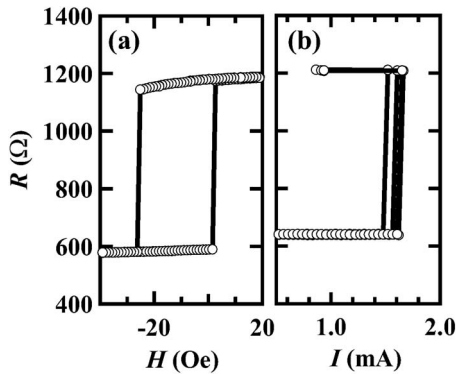


FIG. 1. (a) Minor loop of MR curve and (b) the corresponding pulsed current vs resistance ( $I$ - $R$ ) curve at RT. The MR ratio, offset field, and coercive force obtained from the MR curve were, respectively, 115%, -13 Oe, and 15 Oe. In the  $I$ - $R$  curve, a 20 ns pulse duration current was used; five times switching events are shown.

measurement time range because sufficient rf transmittance was needed in the time range 2–100 ns. We also carried out real-time observation of the STS switching process. This dynamic measurement was performed using a storage oscilloscope with a 40 Gbit/s sampling rate and 12 GHz bandwidth.

### III. RESULTS AND DISCUSSIONS

Figure 1(a) depicts the MR curve of the MTJ measured using a four-probe method. The coercive force  $H_C$  and the offset field are, respectively, 15 and -13 Oe. The MR ratio of 115%, together with the resistance-area product of  $17 \Omega \mu\text{m}^2$ , is sufficient for STS observation. The sharp resistance transition suggests that the free layer magnetization has an almost single-domain structure. Figure 1(b) portrays a pulsed current-resistance ( $I$ - $R$ ) curve using the pulsed current with 20 ns width. Here, the positive current direction was defined as that of the electron flow from the free layer to the pinned layer. A sharp resistance change occurs at around 1.6 mA. The magnitude of the resistance changes is the same between both curves; moreover, the current direction is appropriate for P to AP switching. Therefore, STS was observed in this MTJ.

Figure 2 shows the switching current  $I_C$  for different pulse durations. From 10  $\mu\text{s}$  to 100 ms,  $I_C$  shows an almost linear relation against  $\ln(\tau_p/\tau_0)$ . We fitted these experimental results to a thermal activation model<sup>11,12</sup> expressed as

$$I_C = I_{C0} \{1 - (k_B T/E) \ln(\tau_p/\tau_0)\}. \quad (1)$$

Here,  $I_{C0}$ ,  $k_B$ ,  $T$ ,  $E$ , and  $\tau_0$ , respectively, denote the intrinsic switching current, Boltzmann's constant, temperature, energy barrier, and attempt time, which was assumed as  $1 \times 10^{-9}$  s. Using the fitting,  $I_{C0} = 1.7$  mA and  $E = 32 k_B T$  are obtained. Data points between 10 and 100 ns show an almost straight linear relationship, but the switching current drastically increases and deviates from the line below the 10 ns region. According to this simple analysis, the thermal activation process would be dominant for the magnetization reversal in the  $>10$  ns region; in the  $<10$  ns region, some other processes should be considered. The most plausible model is an adiabatic precessional model,<sup>17,18</sup> expressed as

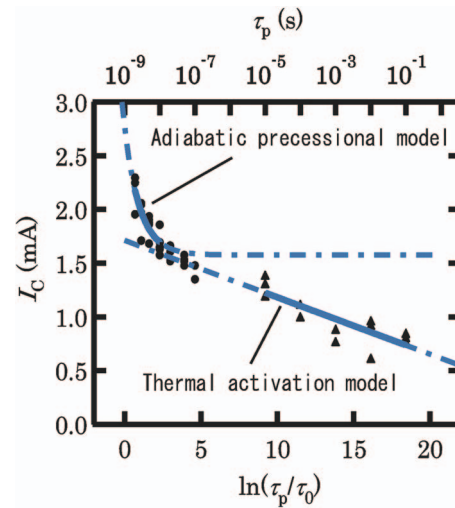


FIG. 2. (Color)  $I_C$  depending on the pulse width. Marks show the experimental points corresponding to 2–100 ns ( $\bullet$ ) and 10  $\mu\text{s}$ –100 ms ( $\blacktriangle$ ). Solid lines show the fitting curves based, respectively, on the adiabatic and thermal activation model in the 2–10 ns and 10  $\mu\text{s}$ –100 ms regions. Dashed lines show extrapolations for each fitting curve.

$$I_C = I_{C0} \left\{ 1 + \frac{\tau_{\text{relax}}}{\tau_p} \ln \left( \frac{\pi/2}{\theta_0} \right) \right\}, \quad (2)$$

where  $\tau_{\text{relax}}$  and  $\langle \theta_0 \rangle$ , respectively, represent the relaxation time and root square average of the initial angle of the free layer magnetization, which is determined by thermal fluctuation. Data in the 2–10 ns region can be fitted well to this model. By assuming  $\langle \theta_0 \rangle = \sqrt{k_B T/2E} = 0.13$ ,  $I_{C0} = 1.6$  mA and  $\tau_{\text{relax}} = 3.0 \times 10^{-10}$  s are obtained as fitting parameters. It is noteworthy that  $I_{C0}$  from the independent models show good agreement. Similar analysis has already been reported for CPP-GMR (Refs. 11, 14, 16, and 17) and MgO-MTJ.<sup>10,13</sup> However, we should be careful for considering the contribution of high frequency loss.

Here, we discuss the increase of switching current less than 10 ns, where relatively few thermal attempts are permitted. Using the static pulsed current versus resistance measurement, the switching characteristics in the nanosecond region are shown; they are explainable using the same model in CPP-GMR cases.<sup>11,14,16,17</sup> However, this increment of  $I_C$  in the nanosecond region can also be explained by high frequency signal loss in the measurement system and the electrode. We analyzed high frequency transmittance characteristics for our measurement system including sample using a vector network analyzer between dc and 20 GHz to ascertain the effect on our MTJs. For this analysis, we used the equivalent circuit of our measurement system and the sample to reproduce the pulsed current shape flowing into the MTJ. In the  $>1$  ns pulse duration case, results showed that the decay of the magnitude of the pulsed current was negligible. The rise time of the pulse in our setup is about 0.5 ns, which is sufficient to measure the fast-switching properties in this case. Consequently, we can conclude that the drastic increment of  $I_C$  in the nanosecond region is reflected in the MTJ property. However, in the subnanosecond case, the current decay attributable to the high frequency transmittance limit

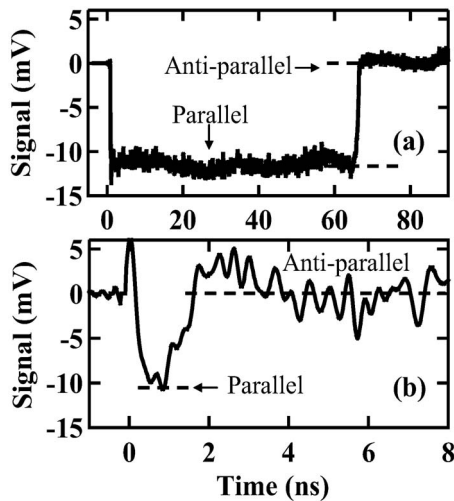


FIG. 3. Voltage signals attributable to the free layer magnetization reversal from parallel to antiparallel configuration using (a) 1.5 and (b) 2.4 mA step currents in real time. Low and high voltage levels correspond to the parallel and antiparallel magnetization configurations. For measurement of (b), we used bandwidth limitation for the switching signal to 3 GHz to achieve noise reduction.

cannot be negligible. Improvement of the high frequency transmittance of the measurement system is necessary for subnanosecond STS measurement.

Moreover, consideration must be given to the limitation of the thermal activation model<sup>11,12</sup> for experimental data analysis. This model is assumed only in the case of  $I_{C0} \gg I_C$ . Moreover, the Boltzmann energy distribution will break when the  $I_C$  is both close to  $I_{C0}$  and above  $I_{C0}$ .<sup>25</sup> The use of this theory can also give rise to a gradual increase of  $I_C$  from the linear relationship to  $\ln(\tau_p/\tau_0)$  in the short pulse width region, where  $I_C$  is both close to  $I_{C0}$  and above  $I_{C0}$ . We could not find this contribution to the  $I_C$  on each  $\tau_p$  at this stage. Actually,  $I_C$  on each  $\tau_p$  in the nanosecond region might be determined by both precession amplification<sup>18</sup> and with thermal fluctuation<sup>25</sup> pictures.

Additional knowledge related to fast STS is provided by real-time observation of the switching event. This measurement is expected to reflect magnetization dynamics clearly; it can clarify the detailed switching mechanism directly whether it is adiabatic, thermally activated, or via some intermediate resistance state (e.g., vortex, multidomain, or precession).

Figure 3 shows results of time-dependent measurements for (a) 1.5 mA ( $< I_{C0}$ ) and (b) 2.4 mA ( $> I_{C0}$ ) step currents applied to the MTJ in a parallel magnetization configuration under  $H_{\text{eff}}=0$ . The horizontal axis shows the time from when the rising voltage reaches half of its equilibrium level. The background signal, which was traced in the AP configuration under the same effective field, was subtracted from the signal in the P configuration. High and low voltage levels correspond, respectively, to the AP and P states; the initial voltage drop is caused by the pulse onset. After the switched region in (b), the signal was oscillating. However, this is inferred to be noise because the measurement system does not reflect magnetization dynamics.

As Fig. 3(a) shows, free layer magnetization remains in

a parallel state after the pulse onset for about 60 ns, with subsequent abrupt switching of the transition time of a few nanoseconds. The endurance time after the pulse onset changed at every single shot, with a few tens of nanoseconds' deviation, despite the identical measurement condition. This phenomenon is characterized qualitatively by the thermal activation model.<sup>11,12</sup> During the P state after the pulse onset, spin transfer torque is imparted on the free layer, thereby pumping its magnetization. However, spin torque of less than the damping torque causes a small magnetization precession;<sup>18</sup> for that reason, magnetization reversal never occurs without an extrinsic excitation such as the thermal excitation. On the other hand, as depicted in Fig. 3(b), magnetization reversal occurs rapidly immediately after the pulse onset. It apparently occurs because of the current itself. In the adiabatic precessional model, magnetization reversal occurs via precession amplification by spin transfer torque, which is greater than the damping torque. The contribution of thermal activation to the switching event is relatively small because the speed of the angle amplification by a larger current would be fast.<sup>18</sup> Moreover, Finocchio *et al.*<sup>26</sup> reported collinear magnetization configuration that probably induced reversal via nucleation of a vortex. In our experiments, such an intermediate resistance state did not appear. One reason is that the temperature during the experiment was RT, in which free layer magnetization thermally fluctuated. In this case, coherent magnetization reversal might occur easily.

The switching endurance time from the real-time measurements for several steps of current was the expected value from static measurement results described above. Our real-time measurement showed uniform magnetization rotation in Figs. 3(a) and 3(b). In previous reports<sup>11,16</sup> of CPP-GMR using a sampling oscilloscope, the signal was averaged by several tens of thousands of events so that it became a gradual transition. In this work, we were unable to clarify precession amplification by spin torque. Through further improvement of measurement techniques, we believe that this motion will eventually be detected. In addition, for MTJs, it has been shown both theoretically<sup>19,20</sup> and experimentally<sup>27,28</sup> that spin transfer efficiency is not constant for bias voltage. In this paper, the current magnitude was as high as 2.4 mA, corresponding to the bias voltage of 1.4 V. Although the wide range of the bias voltage affects the bias-dependent contribution to  $I_C$ , our results of  $I_C$  depending on  $\tau_p$  showed good agreement with analytical models.<sup>11,18</sup> The time-dependent switching process was consistent with these models. Details of the bias-dependent contribution to the  $I_C$  vs  $\tau_p$  must be investigated further to both elucidate the physics and devise applications.

#### IV. CONCLUSIONS

We investigated STS in the nanosecond-switching-speed region for MgO-based MTJ using static and dynamic measurements. Using static measurements, we detected a drastic increase of  $I_C$  in the few nanoseconds region and confirmed that the characteristics were not explained by the decrease of pulsed current amplitude caused by high frequency loss.

However, theoretical limitation of the thermal activation model contributed to the  $I_C$  increment in the short pulse width region. Additionally, we observed real-time STS from P to AP configurations. For application of current larger than  $I_{C0}$ , which corresponds to  $\tau_p$  of  $\sim 1$  ns, switching events qualitatively showed adiabatic characteristics, whereas switching occurred with assistance by thermal activation at currents of less than  $I_{C0}$ .

## ACKNOWLEDGMENTS

This study was supported by the “High-Performance Low-Power Consumption Spin Devices and Storage Systems” program under Research and Development for Next-Generation Information Technology by the Ministry of Education, Culture, Sports, Science and Technology of Japan.

- <sup>1</sup>S. Yuasa, A. Fukushima, Y. Suzuki, and K. Ando, *Nat. Mater.* **3**, 868 (2004).
- <sup>2</sup>S. S. P. Parkin, C. Kaiser, A. Panchula, P. M. Rice, B. Hughes, M. Samant, and S.-H. Yang, *Nat. Mater.* **3**, 862 (2004).
- <sup>3</sup>D. D. Djayaprawira, K. Tsunekawa, M. Nagai, H. Maehara, S. Yamagata, N. Watanabe, S. Yuasa, Y. Suzuki, and K. Ando, *Appl. Phys. Lett.* **86**, 092502 (2005).
- <sup>4</sup>J. C. Slonczewski, *J. Magn. Magn. Mater.* **159**, L1 (1996).
- <sup>5</sup>L. Berger, *Phys. Rev. B* **54**, 9353 (1996).
- <sup>6</sup>J. C. Slonczewski, *Phys. Rev. B* **71**, 024411 (2005).
- <sup>7</sup>H. Kubota, A. Fukushima, Y. Ootani, S. Yuasa, K. Ando, H. Maehara, K. Tsunekawa, D. D. Dyayaprawira, N. Watanabe, and Y. Suzuki, *Jpn. J. Appl. Phys., Part 2* **44**, L1237 (2005).
- <sup>8</sup>J. Hayakawa, S. Ikeda, Y. M. Lee, R. Sasaki, T. Meguro, F. Matsukura, H. Takahashi, and H. Ohno, *Jpn. J. Appl. Phys., Part 2* **44**, L1267 (2005).
- <sup>9</sup>Z. Diao, D. Apalkov, M. Pakala, Y. Ding, A. Panchula, and Y. Huai, *Appl. Phys. Lett.* **87**, 232502 (2005).

- <sup>10</sup>M. Hosomi, H. Yamamoto, K. Bessho, Y. Higo, K. Yamane, H. Yamada, M. Shoji, H. Hachino, C. Fukumoto, H. Nagao, and H. Kano, *Tech. Dig.-Int. Electron Devices Meet.* **2005**, 459.
- <sup>11</sup>R. H. Koch, J. A. Katine, and J. Z. Sun, *Phys. Rev. Lett.* **92**, 088302 (2004).
- <sup>12</sup>Z. Li and S. Zhang, *Phys. Rev. B* **69**, 134416 (2004).
- <sup>13</sup>M. Hosomi, T. Yamamoto, Y. Higo, K. Yamane, Y. Oishi, and H. Kano, *Trans. Magn. Soc. Jpn.* **2**, 606 (2007).
- <sup>14</sup>A. A. Tulapurkar, T. Devolder, K. Yagami, P. Crozat, C. Chappert, A. Fukushima, and Y. Suzuki, *Appl. Phys. Lett.* **85**, 5358 (2004).
- <sup>15</sup>S. Kaka, M. R. Pufall, W. H. Rippard, T. J. Silva, S. E. Russek, J. A. Katine, and M. Carey, *J. Magn. Magn. Mater.* **286**, 375 (2005).
- <sup>16</sup>I. N. Krivorotov, N. C. Emley, J. C. Sankey, S. I. Kiselev, D. C. Ralph, and R. A. Buhrman, *Science* **307**, 228 (2005).
- <sup>17</sup>T. Devolder, P. Crozat, J.-V. Kim, C. Chappert, K. Ito, J. A. Katine, and M. J. Carey, *Appl. Phys. Lett.* **88**, 152502 (2006).
- <sup>18</sup>J. Z. Sun, *Phys. Rev. B* **62**, 570 (2000).
- <sup>19</sup>P. M. Levy and A. Fert, *Phys. Rev. Lett.* **97**, 097205 (2006).
- <sup>20</sup>I. Theodonis, N. Kioussis, A. Kalitsov, M. Chshiev, and W. H. Butler, *Phys. Rev. Lett.* **97**, 237205 (2006).
- <sup>21</sup>M. R. Pufall, W. H. Rippard, S. Kaka, S. E. Russek, T. J. Silva, J. A. Katine, and M. Carey, *Phys. Rev. B* **69**, 214409 (2004).
- <sup>22</sup>I. N. Krivorotov, N. C. Emley, R. A. Buhrman, and D. C. Ralph, *Phys. Rev. B* **77**, 054440 (2008).
- <sup>23</sup>T. Devolder, J. Hayakawa, K. Ito, H. Takahashi, S. Ikeda, J. A. Katine, M. J. Carey, J. Kim, C. Chappert, and H. Ohno, 52nd MMM Conference on BB-08, 2007 (unpublished).
- <sup>24</sup>T. Aoki, D. Watanabe, T. Daibou, Y. Ando, M. Oogane, and T. Miyazaki, *J. Magn. Soc. Jpn.* **31**, 94 (2007) (in Japanese).
- <sup>25</sup>P. B. Visscher and D. M. Apalkov, *J. Appl. Phys.* **99**, 08G513 (2006).
- <sup>26</sup>G. Finocchio, I. N. Krivorotov, L. Torres, R. A. Buhrman, D. C. Ralph, and B. Azzerboni, *Phys. Rev. B* **76**, 174408 (2007).
- <sup>27</sup>J. C. Sankey, Y.-T. Cui, J. Z. Sun, J. C. Slonczewski, R. A. Buhrman, and D. C. Ralph, *Nat. Phys.* **4**, 67 (2008).
- <sup>28</sup>H. Kubota, A. Fukushima, K. Yakushiji, T. Nagahama, S. Yuasa, K. Ando, H. Maehara, Y. Nagamine, K. Tsunekawa, D. D. Djayaprawira, N. Watanabe, and Y. Suzuki, *Nat. Phys.* **4**, 37 (2008).